Appendix 7

ICE CLOUD AND BACKGROUND WATER VAPOUR BY SUB-MM AND VERY-HIGH FREQUENCY MW RADIOMETRY

By: Klaus Künzi, Georg Heygster and Jungang Miao, University of Bremen

1. Introduction

The purpose of this study is to provide scientific evidence of the mission requirements adopted for the CLOUDS project in relation to the use of sub-millimetre and very-high frequency MW radiometry for observing cloud ice and other cloud characteristics as inferred by water vapour bands. The following discussions will be focused on the rationale of selecting channels in the sub-millimetre and millimetre range including those near the water vapour resonance line at 183.31 GHz.

2. The sub-millimetre channels (463, 683, 874 GHz)

2.1 The scientific background of using sub-millimetre channels for cirrus clouds measurements

Cirrus clouds can be found from the tropics to polar regions in the upper troposphere and lower stratosphere. They consist of ice crystals of various shapes. Information on cirrus cloud parameters (coverage, height, thickness, ice water path, ice particle shape and size distributions) is crucial to the development of cirrus cloud forecast models, the upgrading of real-time global cloud analysis, and the investigation of cloud feedback in global climate change (Liou 1986; Liou et al. 2000). In situ observations of the microphysical properties of cirrus clouds in the last two decades reveal that the ice water content can vary from less than 10^{-4} gm^{-3} to greater than 10^{-1} gm^{-3} and that ice crystals show diverse shapes with sizes ranging from smaller than 20 μm to larger than 2000 μm (Heymsfield 1975; Brown 1993; Noone et al. 1993; McFarquhar and Heymsfield 1996; Goodman et al. 1998; Lawson et al. 1998). Recent measurements have shown that the ice crystal size spectrum can be parameterised in terms of the ambient temperature and the ice water content (Heymsfield and Platt 1984; McFarquhar and Heymsfield 1997). For tropical cirrus, the parameterisation of McFarquhar and Heymsfield (1997) using the combination of a first-order gamma function describing ice crystals smaller than 100 μm and a lognormal function describing larger particles was found to be accurate in estimating ice mass, area and number of particles and in predicting the optical properties of cirrus. Remote sensing approaches for cirrus measurements using both active and passive sensors has been extensively studied. Lidar and Radar have shown their effectiveness in detecting cloud base and top height and in measuring cirrus vertical structure (Sassen 1994; Matrosov 1997). Passive sensors onboard aircraft and satellites, especially those working in visible and infrared bands, have been widely used in measuring cirrus cloud temperature, optical thickness and characteristic particle size (Ou et al. 1993, 1998; Francis et al. 1998; Han et al. 1999). Nevertheless, it is well known that none of the presently available approaches is capable to measure all parameters of cirrus clouds and that combinations of different approaches or new techniques are needed.

Recently, sub-millimetre radiometric measurements from satellites or aircraft in the frequency range of 300-1000 GHz (i.e. wavelength: 1.0-0.3 mm) has been proposed to investigate cirrus clouds (Evans and Stephens 1995a, b; Evans et al. 1998, 1999). Since water vapour absorption is strong within this band, the lower atmosphere is in most cases opaque to the sub-millimetre radiation, so that the surface and low clouds do not affect the upwelling radiation. In addition, ice particles are only weak absorbers, and consequently emit very little sub-millimetre radiation, making the physical temperature of cirrus clouds unimportant to radiometric measurements. Because the wavelength in this band is comparable with the size of ice particles in cirrus, the scattering effect lies within Rayleigh and Mie regimes. As a result, the extinction of cirrus and consequently its radiometric signal are proportional to the volume (mass) of ice particles and, at the same time, sensitive to the ice particle size. Also, the upwelling sub-millimetre radiance does not saturate for most cirrus clouds and the radiative transfer is in its linear regime. In simulations Evans et al. (1998) found that the brightness temperature depression due to the presence of cirrus for a down-looking radiometer is closely related to the ice water path and that the mean size of ice crystals can be estimated using the ratio of brightness temperature depressions measured at two frequencies. These simulations performed at two orthogonal polarisations (vertical and horizontal) further demonstrate that the depolarisation effects of horizontally oriented non-spherical ice particles might be useful in determining the ice particle shape, although the fact that realistic cirrus clouds contain a mixture of ice crystals with different shapes and sizes may limit the applicability of this technique. Evans et al. (1998) suggested, among others, that a sub-millimetre radiometer dedicated to the investigation of cirrus clouds should have multiple channels in order to cover a wide range of total columnar ice and particle sizes and it should include a 183 GHz channel for determining the atmospheric background emission. As a result, four channels at 183±1.6, 495, 665 and 890 GHz are recommended (Evans et al. 1998).

More recently, radiometric measurements from aircraft were carried out by Wang et al. (1998b, 1999). By using radiometers operating at frequencies from 89 up to 340 GHz, they found that the brightness temperature depression caused by cirrus increases dramatically with frequency and that, at frequencies below 200 GHz, significant depressions occurred only in intense cloudy cases (e.g. cirrus with ice water path of 300 gm^{-2}). The study of Wang et al. (1998b, 1999) also revealed that it is necessary to have multi-channel measurements at frequencies higher than 340 GHz in order to retrieve cloud parameters in a wide range. Especially, Wang et al. (1999) showed the importance of a precise and coincident measurement of the background emissions, of particular importance in cases of thin cirrus with small ice particles.

In determining the sub-millimetre channels for a radiometer onboard CLOUDS, we generally accept the four channels proposed by Evans et al. (1998). But, it is necessary to finely tune the channel frequencies in order to improve the quality of the atmospheric background emission measurements. To this purpose, we will consider the matching of the temperature weighting functions of the four channels and the influence of the atmospheric ozone resonance.

2.2 Weighting function matching

Since the four frequencies suggested by Evans (1998) are far away from oxygen absorption lines, the atmospheric radiation in clear sky is dominated by atmospheric water vapour emission. When cirrus clouds appear, the ice particles at high attitudes will scatter the upwelling radiation away from the radiometer viewing direction, causing a reduction in the received radiance. It is this reduction, which is usually expressed by the brightness temperature depression DT_b,

$$DT_b = T_b - T_{b,0}\,, \tag{1}$$

that is directly related to the cirrus cloud parameters. T_b is the measured brightness temperature in case of the cirrus cloud, $T_{b,0}$ is the so-called background emission, which corresponds to the brightness temperature that would be measured without the cirrus cloud. Therefore, precise estimation of this background emission is crucial for the retrieval of cirrus parameters. Measurements of Wang et al. (1998b, 1999) showed that, in most cases, cirrus clouds have only a small effect at frequencies lower than 200 GHz. Therefore, a channel near the strong water vapour absorption line at 183.31 GHz is well suited to measure this background emission, because this channel can be well matched in clear sky situations with high frequency channels if its passbands are properly selected. Here, 'matching' means the two channels sense the same layer of the atmosphere, i.e. they measure the same brightness temperature for a cirrus free situation.

To quantitatively describe the degree of a 'match', the concept of effective temperature sensing height is used. For a down-looking radiometer aboard a satellite, the measured brightness temperature, T_b, is expressed as

$$T_b(f,q)=e_s(f,q)T_s\,¡\,(f,q)+\int_0^H W_T(f,q,z)T(z)dz\ , \qquad (2)$$

in which $W_T(f, q, z)$ is the "temperature weighting function". We define the effective temperature sensing height, denoted by h_e, as

$$h_e(f,q)=\frac{\int_0^H zW_T(f,q,z)dz}{\int_0^H W_T(f,q,z)dz}\ . \qquad (3)$$

In the above equations, f is the frequency and q is the ground surface incidence angle for the viewing direction of the radiometer, e_s and T_s are the surface emissivity and temperature, respectively. ¡ is the transmissivity of the atmosphere. $T(z)$ represents the temperature profile of the atmosphere, the top height of which is denoted by H. Note that h_e defined here is different from that defined by Klein and Gasiewski (1998), who used the so-called incremental weighting function. According to ***Eq. (3)***, h_e is the "centre-of-gravity" location of the temperature weighting function, which is normally close to the position of the weighting function maximum. An ideal match between two channels implies that their h_e remains equal under all atmospheric conditions. In reality, however, such an ideal match is impossible, because the vertical structure of atmospheric water vapour and temperature is subject to strong temporal and spatial fluctuation, and the water vapour absorption (or emission) in the sub-millimetre range has a considerable temperature dependency which, in turn, is a function of frequency. Moreover, the available water vapour absorption models at frequencies above 500 GHz contain significant uncertainties in atmospheric windows (Buehler 1996).

Nevertheless, weighting function matching based on Liebe's model (Liebe 1989) were carried out using MWMOD (MicroWave MODel), a radiative transfer software package developed by Simmer (1994). Six standard atmospheres, which are supported by MWMOD, were used in these calculations. They represent subtropical summer, tropical, mid-latitude summer and winter, US standard, and sub-arctic winter. The integrated columnar water vapour or the total water vapour (TWV) corresponding to the six atmospheres are respectively 42.76, 42.55, 29.53, 21.24, 14.50, 8.81 kgm^{-2}. Since TWV values in general decrease with increasing latitude, we will use TWV as a rough indication of latitude. For the four channels suggested by Evans et al. (1998), calculations show that the two lower frequency channels (183.31±1.6 GHz and 495 GHz) sense approximately one kilometre higher than the two higher frequency channels (665 GHz and 890 GHz) (see ***Fig. 1***). To improve the matching, one has to make some adjustments, either on the two lower or on the two higher frequency channels. One of the best matched groups of channels is found near 183.31±2.4, 462, 682, and 878 GHz. The temperature weighting functions for this group of channels, calculated for the US standard atmosphere are shown in ***Fig. 2***. The effective temperature sensing heights at the four selected frequencies are shown in ***Fig. 3*** for the six standard atmospheres in terms of TWV. The h_e at q=50^o is approximately 0.8 km higher than for q=0^o for all frequencies; and for both incidence angles (0^o and 50^o) the h_e is a few kilometres lower than the tropopause. Generally, h_e increases with increasing water vapour (i.e. with decreasing latitude), from approximately 5.0 km in the sub-arctic to 7.0 km in the tropic for q=50^o. This feature is consistent with the general trend of global cirrus cloud distributions (Wang, P.-H. et al. 1996). The maximum difference of h_e for same incidence angle and same atmosphere is less than 300 m, indicating a good match among the four frequencies. In ***Fig. 4***, the clear sky T_b modelled at the three high frequency channels is plotted against T_b modelled at 183.31±2.4 GHz. For most cases, T_b (high frequency) departs from T_b(183.31

GHz) no more than 1.0 K, except for the case of a sub-arctic atmosphere with q=0^o (indicated by the three column outliers with T_b(183.31 GHz)≈248 K), where the water vapour amount in the atmosphere is low and the 183.31±2.4 GHz channel already sees the surface. In fact, the frequency dependent surface emission will be a problem in polar regions, where the atmosphere is so dry that the ground surface emission will play a role. In this case, the differences in surface emissivity and in the degree of 'seeing' the ground at the four channels will make it difficult to predict the background emission using the 183.31 GHz measurements.

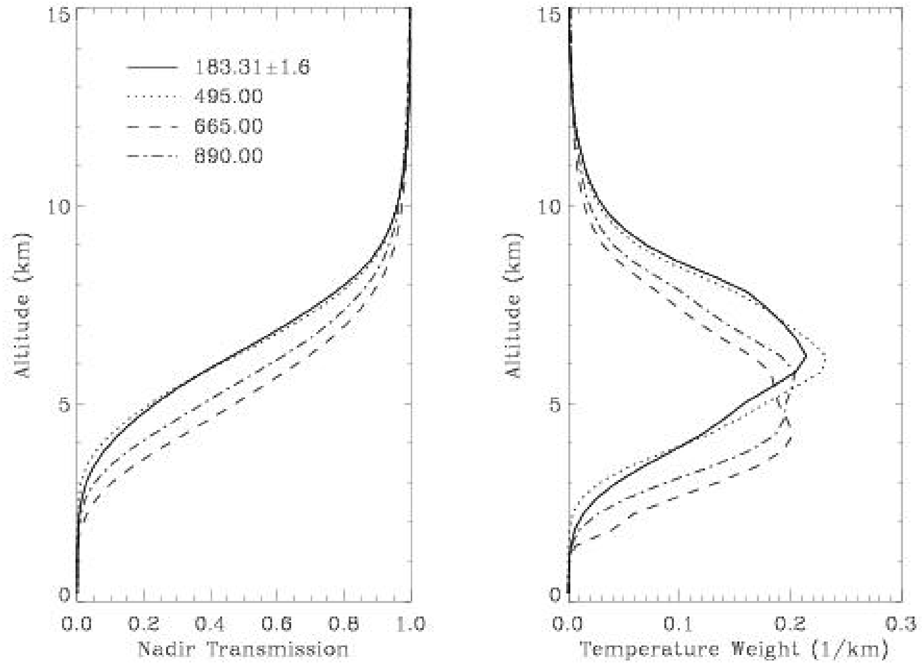

Fig. 1 - ***The temperature weighting functions for the US standard atmosphere at the four frequencies recommended by Evans et al. (1998).***

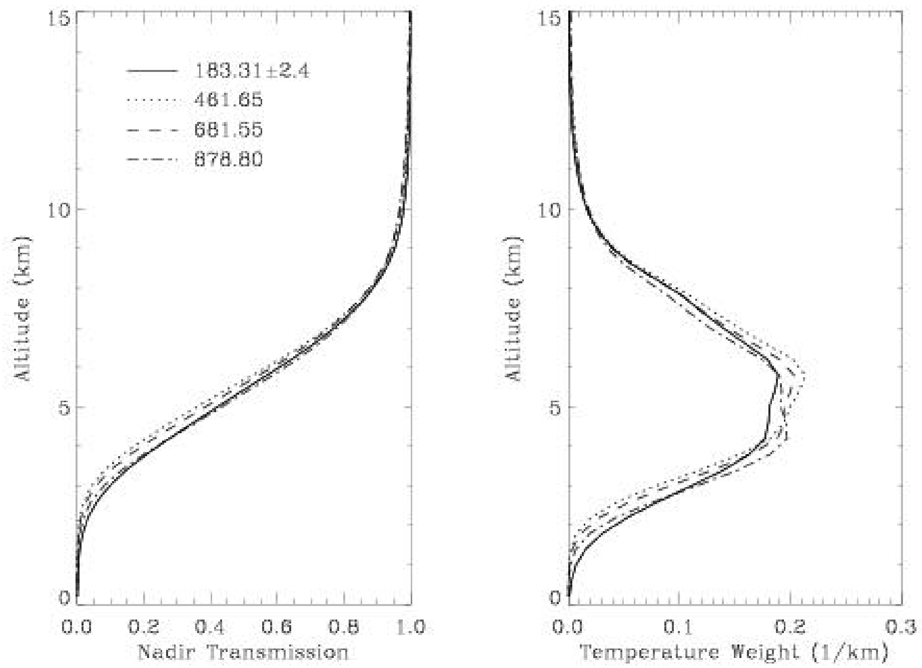

Fig. 2 - ***The temperature weighting functions for the US standard atmosphere at the four frequencies which are found for a best match and are therefore proposed for CLOUDS .***

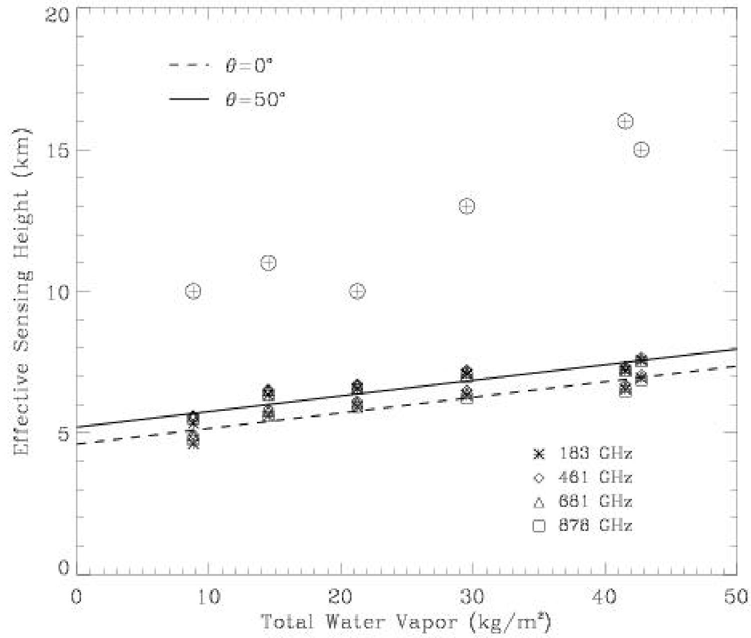

Fig. 3 - ***The effective temperature sensing heights at the four CLOUDS channels for the six standard atmospheres (sub-tropical summer, tropical, mid-latitude summer and winter, US standard, and sub-arctic winter). The TWV values can be regarded as a rough indicator of latitude. The height of the tropopause for each standard atmosphere is denoted using the symbol ⊕. The solid lines show the linear fits of h_e in terms of TWV.***

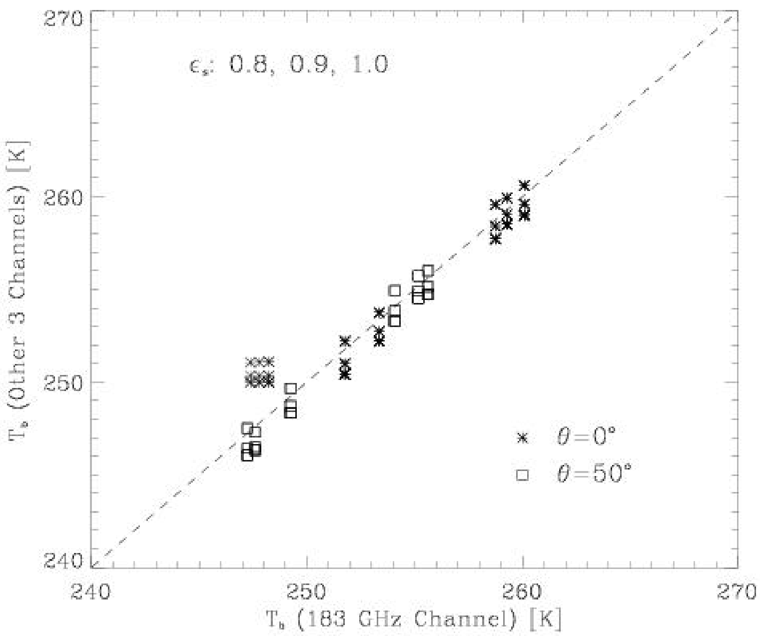

Fig. 4 - ***The clear sky T_b, i.e. the background emission from atmospheric water vapour, at the three sub-millimetre channels versus the T_b at the 183 GHz channel. In most cases, the high frequency background can be precisely estimated from the 183 GHz measurements, except for the case of the sub-arctic atmosphere with $q=0^o$, indicated by the three columns "*" departing from the diagonal line.***

2.3 Minimising ozone influence

Ozone (O_3) is one the most important trace gases that may considerably influence satellite radiometric measurements in the sub-millimetre range. The altitude profile of the O_3 mixing ratio in the atmosphere exhibits a complex structure, but with most O_3 concentrating in the altitude range of 15-50 km, i.e. from the upper troposphere through the stratosphere to the lower mesosphere. Due to the temperature inversion above the tropopause up to the stratopause, where the temperature may reach 280 K, the ozone layer affect the measurements of a spaceborne radiometer in a way that is related to the intensity of the up-welling radiation from troposphere. Since the four channels selected for CLOUDS cover a large range of frequencies, the influence of atmospheric ozone is expected to significantly vary in the four channels (see ***Fig. 5***). Moreover, both the vertical distribution and the total columnar amount of O_3 fluctuate considerably on various temporal and spatial scales. For example, the root-mean-square of day to day variations of the total column ozone can be as large as 10% of the mean total column ozone in some mid-latitude regions (Allen and Reck 1997); and the spatial variation is expected to be much larger if the low extremes of total column ozone in polar regions (ozone hole) are considered. Since the ozone absorption lines near the 183.31 GHz are significantly weaker than those near the three sub-millimetre channels, the fluctuations of atmospheric ozone will be a considerable error source for the estimation of sub-millimetre background emission using 183.31 GHz measurements. Referring to ***Fig. 5***, the three submillimeter channels are located in flat window regions of water vapour, which implies that a small adjustment on the channel frequency does not significantly impact the effective temperature sensing height, but it can effectively reduce the ozone influence by properly placing the passbands avoiding ozone lines.

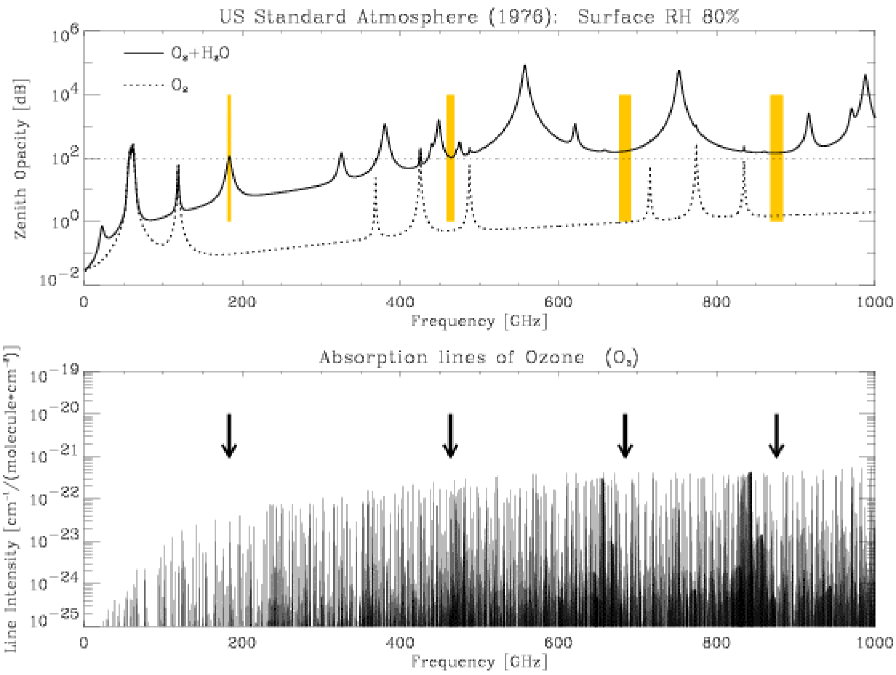

Fig. 5 - ***Locations of the CLOUDS sub-millimetre channels in relations with the atmospheric oxygen, water vapour (top) and ozone (bottom) within the frequency range of 0-1000 GHz. Ozone data from Rothman et al. (1998).***

For this purpose, simulations were done using a radiative transfer model called FORWARD, developed at the Institute of Environmental Physics, University of Bremen. Standard profiles of ozone, temperature and water vapour for a tropical atmosphere were used. As seen in the example shown in ***Fig. 6***, the disturbance due to ozone absorption can be as large as 10 K in a narrow band of frequency. Even for a radiometer with a wide bandwidth, the ozone disturbance can still be larger than 1.0 K, if strong ozone lines are not avoided (see the bottom plot of ***Fig. 6***). To optimise the channel parameters, the ozone disturbance, dT_b, i.e. the difference between the up-welling T_b with and without ozone, is calculated for proper ranges of the centre frequency f_0 and the intermediate frequency f_{IF} under the condition that a pre-selected bandwidth *Df* has been provided by engineers in filter design. The optimal f_{IF} is determined by engineers in filter design and finally the optimal f_0 is selected in the minimum region of T_b (see ***Figs. 7-9***). ***Fig. 10*** shows the case for the 183.31 GHz channel, for which no optimisation needs to be done, since its f_0 and f_{IF} have been fixed by the weighting function matching procedure.

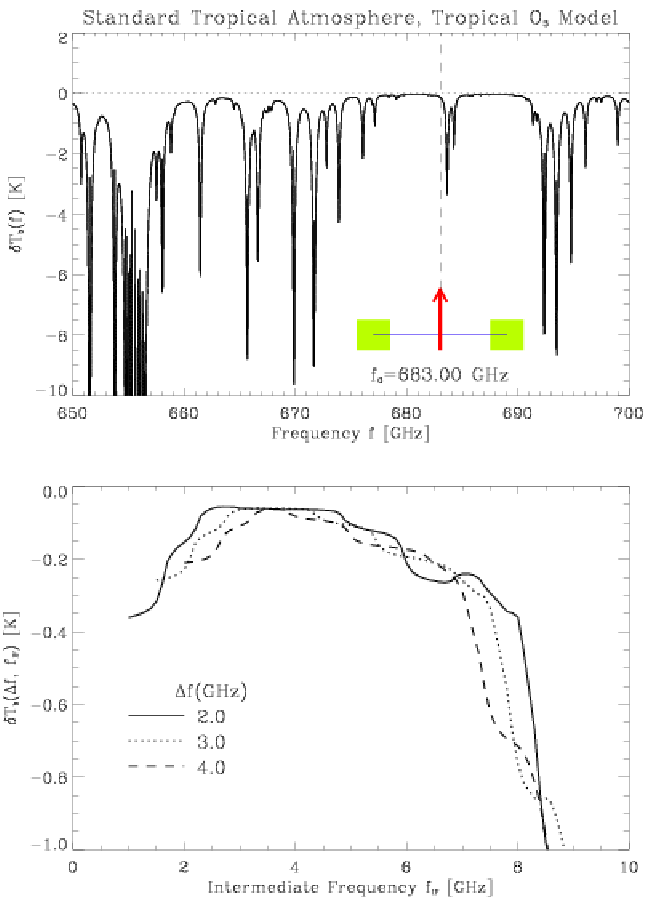

Fig. 6 - **Top*****: The absorption lines of ozone around 683 GHz, dT_b represents the influence of ozone, which is calculated as the difference between the upwelling T_b at the top of the atmosphere with and without the ozone layer.*** **Bottom*****: The ozone influence for a radiometer centred at 683.0 GHz with a passband width Df (indicated by the grey squares in the top plot) and an intermediate frequency $f_{IF.}$***

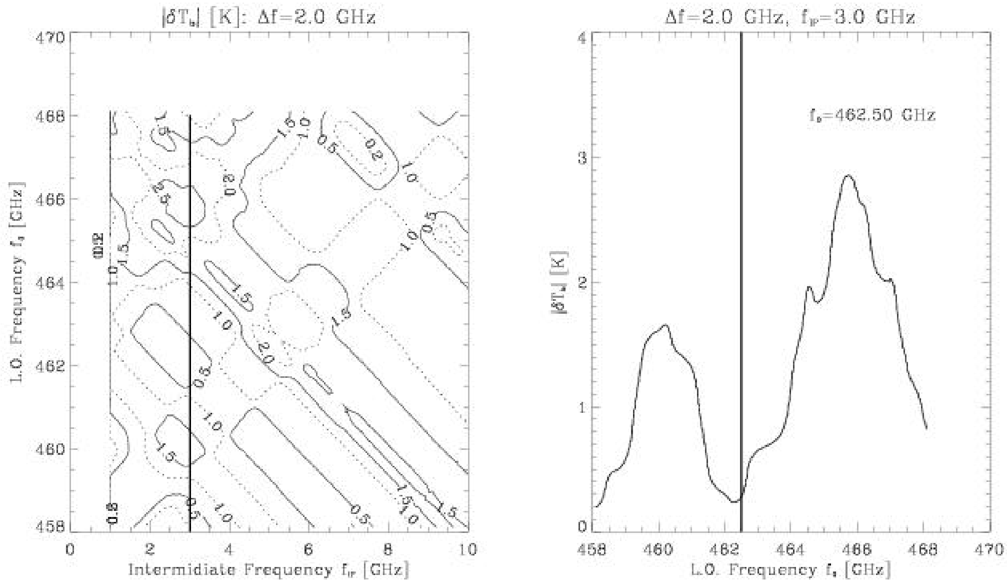

Fig. 7 - **Left*****: The ozone influence ½dT_bï for a receiver with a bandwidth Df (pre-selected here as 2.0-GHz) for a changing centre frequency f_0 and intermediate frequency $f_{IF.}$. The vertical line indicates a proper value of $f_{IF.}$ which is achieved by an appropriate filter design.*** **Right*****: A profile of ½dT_bï as shown in the left, for pre-selected Df and $f_{IF.}$ The optimal centre frequency f_0 can be selected near the minimum of ½dT_bï.***

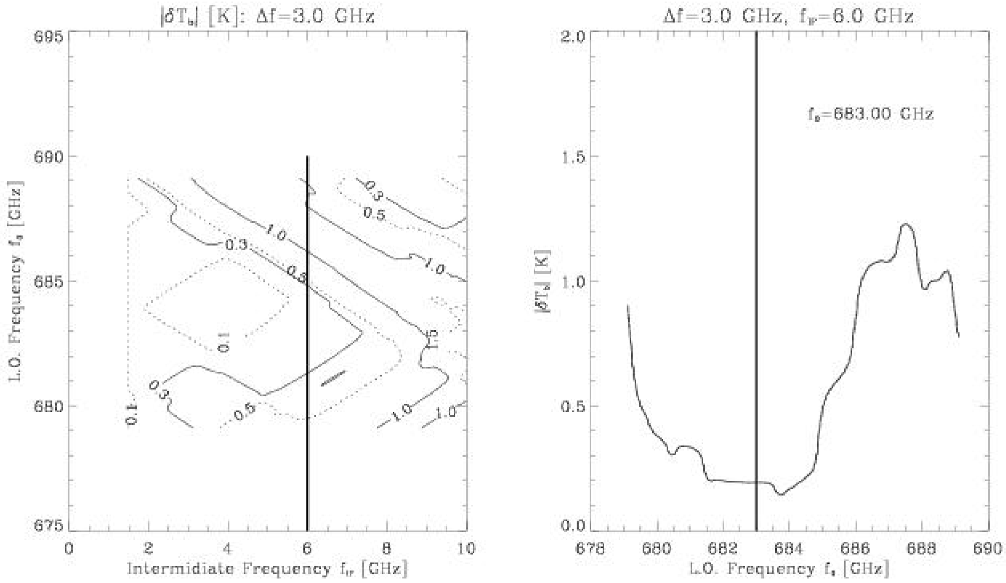

Fig. 8 - ***Same as Fig. 7 but for the channel at 683 GHz.***

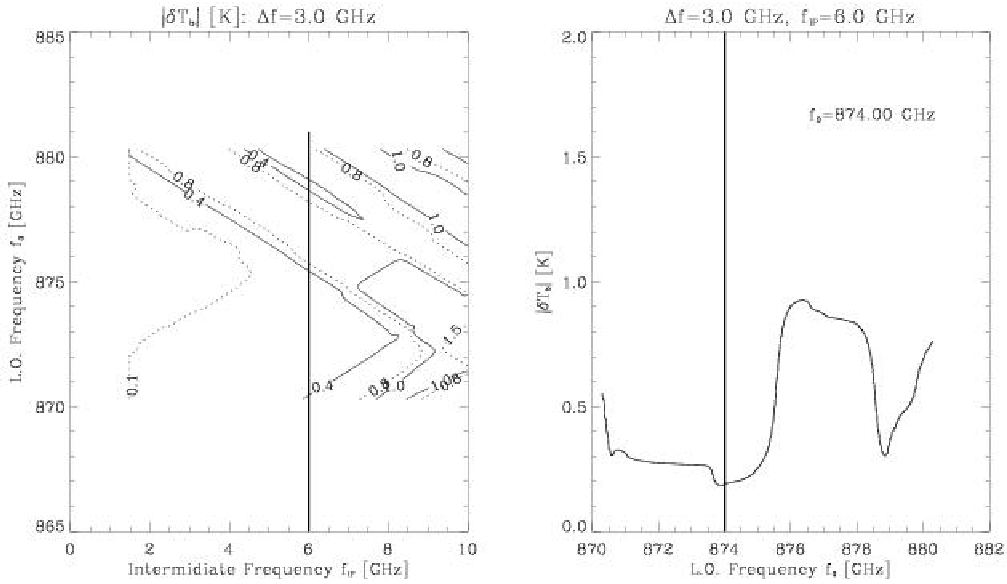

Fig. 9 - ***Same as Fig. 7 but for the channel at 874 GHz.***

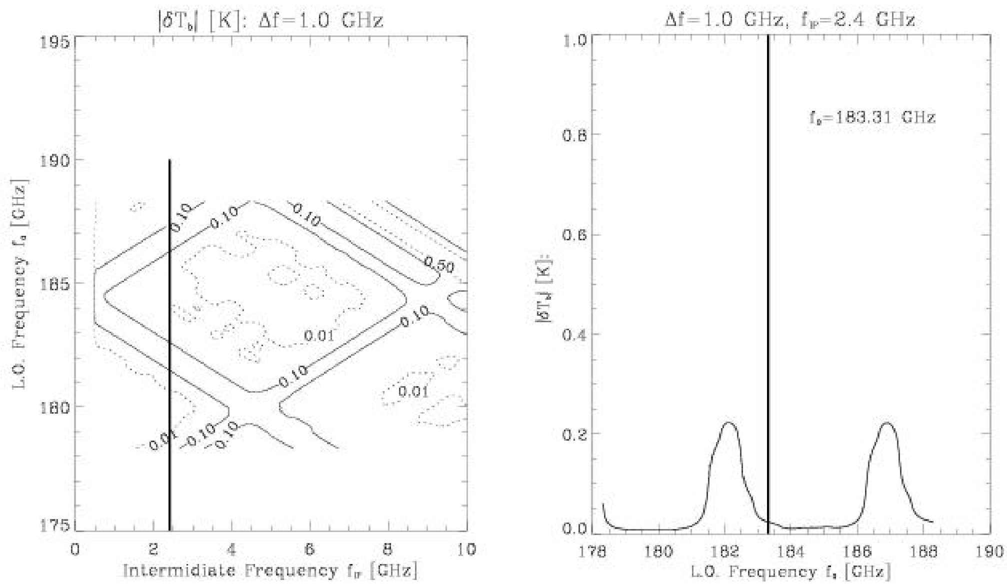

Fig. 10 - ***Similar to Fig. 7 but for the 183 GHz channel for which, in fact, no optimisation of f_0 is needed.***

The purpose of showing it is to give a basic idea on how insignificant the ozone influence is at 183.31 GHz compared with the influence at the other three channels. In summary the channel parameters of the submillimetre radiometer are listed in ***Table 1***.

Table 1 - The sub-millimetre channels

Channel No.	1	2	3	4
f_0 (GHz)	183.31	462.5	683.0	874.0
f_{IF} (GHz)	2.4	3.0	6.0	6.0
Df (GHz)	1.0	2.0	3.0	3.0

2.4 Double sideband receiver

All receivers will operate in a double sideband mode. This design helps to reduce measurement uncertainties caused by frequency instability of the local oscillator (L.O.) and reduces the complexity of the receiver design. Since the two passbands are located either symmetrically across the water vapour line (the 183.31 GHz channel) or in a flat window (the other three sub-millimetre channels), the effect in one sideband due to a L.O. frequency drift will be compensated to a large extent by the corresponding change in the image band. Simulations using the US standard atmosphere show that an L.O. frequency drift of 100 MHz causes the brightness temperature to change less than 0.05 K for all four channels.

3. The millimetre window channels (150.0, 220.5 GHz)

The millimetre channel at 150.0 GHz has been widely used since a number of years in water vapour sounders onboard the DMSP satellites (SSM/T2), and more recently on the latest NOAA satellite (AMSU/B). Such sensors have also been flown on aircraft (e.g. MIR). A large number of simulations, measurements and retrievals at this frequency (e.g. Gasiewski 1992; Liu and Curry 1996) already exists. Above 200 GHz only airborne sensors have been flown so far, e.g. the airborne NASA Millimetre-wave Imaging Radiometer (MIR) is equipped with a 220 GHz channel since 1992 (Racette et al. 1996). The primary use of these two channels is the retrieval of water vapour in the lower troposphere. However, they were soon found also to be very useful in detecting ice particles in clouds (Gasiewski 1992; Liu and Curry 1996, 1998; Wang et al. 1997a, 1998c). Moreover, the work performed by Gasiewski (1992) and Liu and Curry (1998) showed that the 220 GHz channel is probably the most sensitive one for measuring cloud ice associated with strong convections. The suggested specifications of the 150 and 220 GHz channels are given in ***Table 2***. Note that the f_{IF} for the 150 GHz channel is not specified here from the scientific point of view, it can be determined to the convenience of the hardware design of the receiver.

Table 2 - The millimetre window channels

Channel No.	5	6
f_0 (GHz)	150.0	220.5
f_{IF} (GHz)	-	3.0
Df (GHz)	4.0	2.0

4. The water vapour channels (near the 183.31 GHz)

4.1 Water vapour profiling in clear sky situations

Profiling of atmospheric water vapour using the 183.31 GHz water vapour absorption line has been explored extensively in the last two decades. Both theoretical simulations and radiometric measurements from aircraft and satellites have demonstrated the usefulness of the channels located near the 183.31 GHz water vapour line in retrieving water vapour profiles under clear sky conditions (e.g. Wang et al. 1993, 1995,1998a; Wilheit 1990).

4.2 Water vapour profiling in the presence of clouds

Under cloudy conditions, water vapour profiling using measurements near 183.31 GHz has been shown to be problematic. In processing the data from the airborne Advanced Microwave Moisture Sounder (AMMS), operating at 90, 183.31±2, ±5 and ±9 GHz, Lutz et al. (1991) and Wang et al. (1993) found that clouds made the retrievals to diverge. Wang et al. (1993) explained this effect by the poor sensitivity (the NEΔT of AMMR is on the order of 5-6 K, improved to about 1 K when averaged), and the small number of channels. Furthermore the limited information on clouds (e.g. cloud top height and cloud liquid water path) made it difficult to account properly for cloud effects in the retrieval. Using the data from a much improved radiometer, the Millimetre-wave Imaging Radiometer (MIR) which observes at 6 spectral bands (89, 150, 183.31±1, ±3, ±7, and 220 GHz) with a NEΔT less than or equal to 1 K, Wang et al. (1997b) obtained much better retrievals under cloudy conditions. Similarly good results are reported by Wilheit and Hutchison (1997), using SSM/T2 data together with cloud top temperature and water phase (ice or liquid) information obtained from AVHRR.

Nevertheless, the problem to retrieve water vapour profiles in the presence of clouds is far from being solved. One reason is the large absorption of liquid water in clouds at these high frequencies, e.g. the channels near 183 GHz allow not to see through a water cloud with a liquid water path of only 0.2 kgm^{-2}; even for the window channels at 150 and 90 GHz the corresponding weighting functions indicate that the largest contribution is coming from the cloud and not from the water vapour, as shown by Isaacs and Delblonde (1987). This means that we have to accept a clear limitation when retrieving water vapour profiles under cloudy conditions. Wang et al. (1997b) gives a maximum acceptable liquid water path of 0.4 kgm^{-2} for a successful water vapour profile retrieval using the MIR instrument. Another limitation in retrieving water vapour profiles under cloudy conditions is the scattering by frozen hydrometeors. To our knowledge all retrievals reported in the literatures have not considered the influence of scattering in clouds. Although both Wang et al. (1997b) and Wilheit and Hutchison (1997) reported satisfactory retrievals in the presence of cirrus clouds, it is obvious that these clouds were not sufficiently thick to have an appreciable scattering effect.

4.3 The potential to detect strong convections

Although the 183 GHz channels seem not to be useful to retrieve water vapour profiles in the presence of thick clouds, in particular if scattering is of importance, these channels might be important for, e.g. detecting the presence of strong convective clouds (Eyre 1990) and perhaps to quantitatively determine their total columnar ice content.

Measurements of storms performed by Wilheit et al. (1982) using an airborne multichannel 183 GHz radiometer show strong brightness temperature depressions over regions near the storm core. Such depressions in the precipitation region of a frontal system off the west coast of the United States were also observed in the SSM/T2 measurements by Lee (1995), in spite of the much lower spatial resolution of the SSM/T2 compared with the airborne radiometer. It is clear that this depression is related to the scattering in the top layer of clouds. Wang et al. (1997a) further reported that the radiometric signatures measured by the 183 GHz channels over storms are similar to those observed over a clear and fairly dry atmosphere with a cold background and they also found a strong correlation between the integrated columnar ice and the brightness temperature difference between two 183 GHz channels. These observations have an important implication to the characterisation of convective cloud properties using the 183 GHz channels. A possible phenomenon is as follows. For a sufficiently humid atmosphere, the strong absorption of water vapour makes the atmosphere opaque near the 183 GHz line, and therefore the received signal is dominated by the water vapour emission. Due to the significant increase of vapour absorption from the line wings to the line centre , an observation made near the line centre will have a corresponding weighting function with a peak at higher altitudes compared to an observation made in the line wing. Consequently the decreasing atmospheric temperature with increasing altitude causes the measured brightness temperatures to decrease when the observing frequency is approaching the line centre from the wing. For the case of a dry atmosphere with a cold background (due to low surface temperature, low surface emissivity, or both), the situation is reversed. Since the absorption of a dry atmosphere is small, the radiation emitted from the background will be a dominant component in the received signals. Because the background is radiometrically cold, the atmospheric emission will increase the measure brightness temperature. (This is the basis for retrieving total atmosphere water vapour over oceans using a sensor operating near the weak water vapour line at 22.2 GHz). Consequently, when observing the atmosphere from satellite at a frequency near 183.31 GHz, the measured brightness temperature will increase with the approach of the observing frequency to the line centre in the case of a dry atmosphere with a cold background. Therefore, the brightness temperature difference between two channels near 183 GHz will show different sign when measured over a rather humid region (e.g. in the low- and mid-latitudes) and over a strong convective system. Burns et al. (1997) first suggested to make use of this unique feature to detect and screen out convective events before doing water vapour profile retrievals.

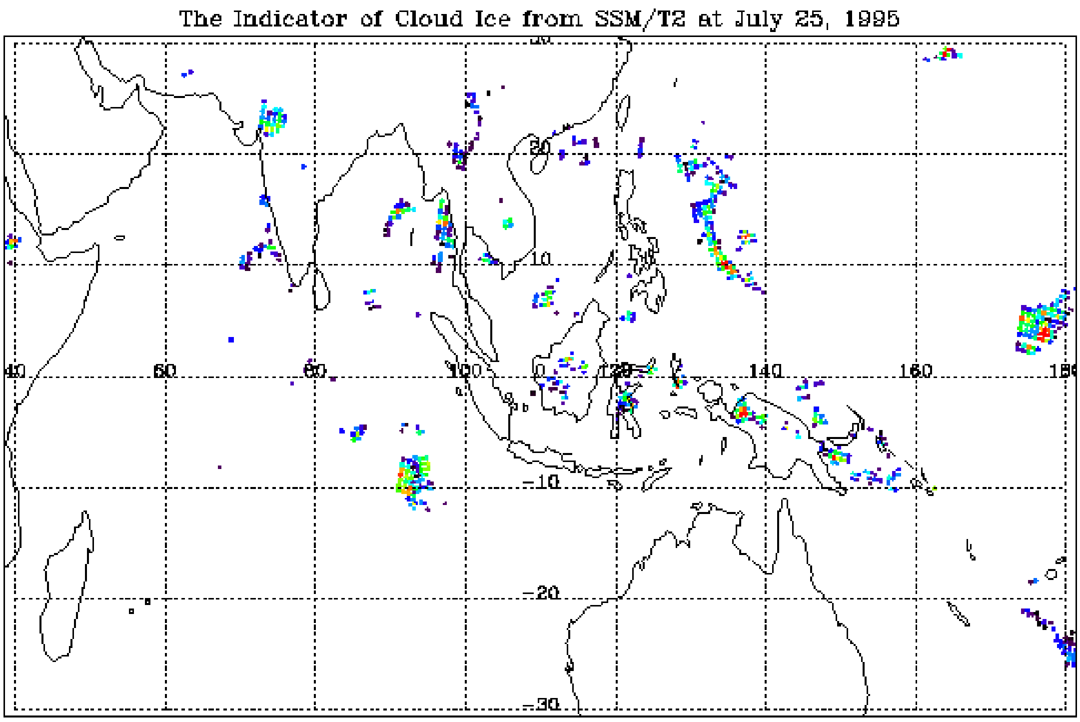

Fig. 11 - ***Cloud ice indicator derived from SSM/T2 measurements near 183.31 GHz. The colour indicates the relative amount of cloud ice, i.e. the integrated cloud ice increases as the colour changes from blue through green to red.***

The possibility of a quantitative use of this specific feature was further explored to retrieve total atmospheric water vapour using the 183 GHz channels (SSM/T2) over the polar ice. Miao (1998) developed an algorithm which is valid for dry polar atmospheres. He successfully applied this technique to obtain for the first time water vapour maps over the Antarctic continent. Since the system comprising a convective cloud layer and a rather dry atmosphere on top is comparable to the case of the Antarctic continent with respect to apparent brightness temperatures, it might be possible to use the same technique to retrieve the water vapour column over a convective cloud. Another important implication of the analysis of Miao (1998) is that the three 183 GHz channels might be used to measure the total columnar ice content within a convective cloud. Using the satellite SSM/T2 data, we found that the maximum value of a "cloud ice indicator" derived from the 183 GHz channel measurements occurs in most cases at the centre of a storm system, which is consistent with the general feature of convective systems described by Houze (1981) (see ***Fig. 11***).

4.4 The influence of the antenna scan geometry

Water vapour sounders such as SSM/T2, AMSU/B and MIR all have three channels at 183.31±1.0, ±3.0 and ±7.0 GHz; and they are working in a cross-track scanning mode. The sounder onboard CLOUDS, however, will operate in a conical scan mode with an Earth surface incident angle of about 50°. Therefore, it is necessary to study if fine tuning is needed for the CLOUDS water vapour channels near 183 GHz.

To understand the influence of the Earth surface incident angle or the satellite zenith angle on the measurements near 183.31 GHz, a statistics of SSM/T2 data at three different incident angles is shown in ***Fig. 12***. For a given frequency, as the antenna scans from the edge position to the nadir direction, the radiometer looks down deeper and deeper into the troposphere. A increase of a few Kelvin in T_b is observed at all three channels when the satellite zenith angle changes from 47.26° to 1.7°, indicating that the radiometer observes approximately one kilometre higher at the antenna scan edge compared to the nadir position. Since the 183 GHz channels onboard CLOUDS will operate with a satellite zenith angle of 50°, they will look not as deep into the atmosphere as the same channels of SSM/T2. The impact of a large satellite zenith angle on the clear sky water vapour retrieval has been studied by McMillin and Divakarla (1999). Their results show that, for the AMSU/B channels, the retrieval with a satellite zenith angle of 50°, in general, gives better results in the upper troposphere when compared to a sounder observing at nadir, due to the lifting and narrowing of the weighting functions. In layers near the surface the results are different for situations over ocean and over land. Over ocean the 50° retrieval is slightly worse than at nadir, while over land there is no noticeable difference. For strong convective clouds, as mentioned earlier, it is the brightness temperature difference (BTD) between neighbouring channels that contains most information on cloud ice. To examine the impact of incidence angle on the BTD, SSM/T2 data were analysed. Our results are shown in ***Fig. 13***. Contrary to the case of a single channel, the BTD does not have a considerable dependency on the incidence angle. This means, the scan geometry is unimportant for BTD. Based on the above analyses, we suggest to keep the water vapour channels of CLOUDS to be consistent with those by SSM/T2 and AMSU/B (see ***Table 3***), because this will facilitate crosschecks between these sensors.

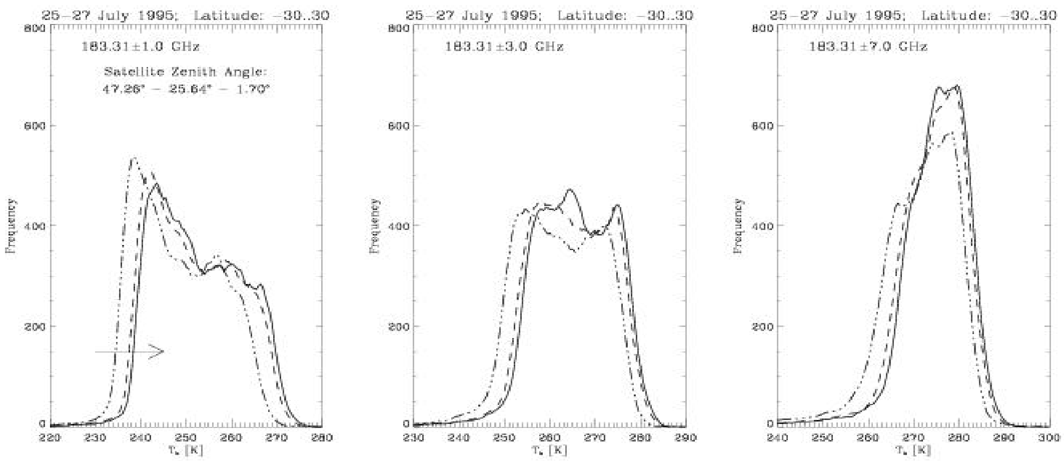

Fig. 12 - ***The shifting (from "cold" to "warm") of the measured brightness temperatures near 183 GHz as the satellite zenith angle changes from an off-nadir to a nadir position .***

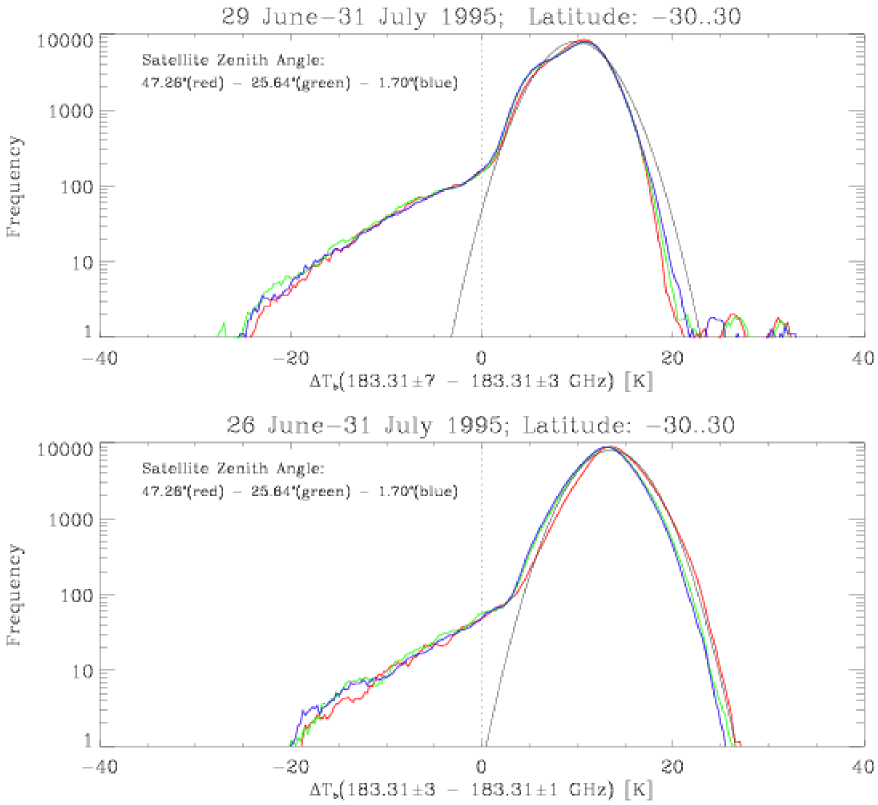

Fig. 13 - ***The distributions of brightness temperature differences between neighbouring channels near 183 GHz for three satellite zenith angles, 47.26°, 25.64°, and 1.70°, which are indicated by the curves in red, green and blue respectively. This statistics is based on an analysis of SSM/T2 data of more than one month. For comparison, a Gaussian distribution (the black curve) is also plotted in each panel.***

Table 3 - The water vapour channels

Channel No.	**7**	**8**	**9**
f_0 (GHz)	183.31	183.31	183.31
f_{IF} (GHz)	1.0	3.0	7.0
Df (GHz)	1.0	2.0	4.0

5. Conclusion

We have discussed the rationale of adopting the sub-millimetre, millimetre window, and water vapour channels near 183 GHz, based on studies published in the literature and on our own analyses. We believe that the suggested channels and their specification are appropriate for CLOUDS. We would like to point out that, since three water vapour channels near 183 GHz are considered to be a crucial element of the millimetre/sub-millimetre package, we suggest to cancel the 183.31±2.4 GHz channel in the sub-millimetre package considered earlier in this study, since the atmospheric background information which is needed by the sub-millimetre channels can be derived from the measurements of the three water vapour channels. Summing up, the mission requirements for sub-millimetre and very-high frequency MW channels are shown in ***Table 4.***

Table 4 - Mission requirements for CLOUDS Sub-mm and very-high frequency MW channels

Channel	Bandwidth (half-power)	Radiometric accuracy	Absolute accuracy	Polarisations	Dual view	IFOV
874.00 ± 6.0 GHz	3.0 GHz	1.0 K @ 240 K	1.5 K	two	required	10 km
683.00 ± 6.0 GHz	3.0 GHz	1.0 K @ 240 K	1.5 K	two	required	10 km
462.50 ± 3.0 GHz	2.0 GHz	1.0 K @ 240 K	1.5 K	two	required	10 km
220.50 ± 3.0 GHz	2.0 GHz	1.0 K @ 240 K	1.5 K	two	required	10 km
183.31 ± 1.0 GHz	1.0 GHz	1.0 K @ 240 K	1.5 K	one	required	10 km
183.31 ± 3.0 GHz	2.0 GHz	1.0 K @ 260 K	1.5 K	one	required	10 km
183.31 ± 7.0 GHz	4.0 GHz	1.0 K @ 280 K	1.5 K	one	required	10 km
150 GHz	4.0 GHz	1.0 K @ 300 K	1.5 K	two	required	10 km

References

Allen D.R. and R.A. Reck, 1997 - Daily variations in TOMS total ozone data - *J. Geophys. Res.*, v.102, pp.13,603-13,608

Brown P.R.A., 1993 - Measurements of the ice water content in cirrus using an evaporative technique - *J. Atmos. Oceanic Technol.*, v.10, pp.579-590

Buehler S., 1996 - The impact of continuum emissions in the mm and sub-mm spectral range - *Final Report to ESA*, IUP, University of Bremen

Burns B.A., X. Wu and G.R. Diak. 1997 - Effects of precipitation and cloud ice on brightness temperatures in AMSU moisture channels - *IEEE Trans. Geosci. Remote Sensing*, v.35, pp.1429-1437

Clancy A.T. and D.O. Muhleman, 1993 - Ground-based microwave spectroscopy of the Earth's stratosphere and mesosphere - *Atmospheric remote sensing by microwave radiometry, ed. M. A. Janssen*, John Wiley & Sons. Inc, pp.335-381

Evans K.F. and G.L. Stephens, 1995a - Microwave radiative transfer through clouds composed of realistically shaped ice crystals. Part I: single scattering properties - *J. Atmos. Sci*., v.52, pp.2041-2057

Evans K.F. and G.L. Stephens, 1995b - Microwave radiative transfer through clouds composed of realistically shaped ice crystals. Part II: remote sensing of ice clouds - *J. Atmos. Sci.*, v.52, pp.2058-2072

Evans K.F, S.J. Walter, A.J. Heymsfield, and M.N. Deeter, 1998 - Modeling of submillimetre passive remote sensing of cirrus clouds - *J. Appl. Meteorol.*, v.37, pp.184-205

Evans K.F, A.H. Evans, I.G. Nolt, and B.T. Marshall, 1999 - The prospect for remote sensing of cirrus clouds with a submillimeter-wave spectrometer - *J. Appl. Meteorol.*, v.38, pp.514-525

Eyre J.R., 1990 - The information content of data from satellite sounding systems: A simulation study - *Q. J. R. Meteorol. Soc.*, v.116, pp. 401-434

Francis P.N., P. Hignett, and A. Macke, 1998 - The retrieval of cirrus cloud properties from aircraft multi-spectral reflectance measurements during EUCREX'93 - *Q. J. R. Meteorol. Soc.*, v.124, pp.1273-1291

Gasiewski A.J., 1992 - Numerical sensitivity analysis of passive EHF and SMMW channels to tropospheric water vapour, clouds, and precipitation - *IEEE Trans. Geosci. Remote Sensing*, v.30, pp.859-870

Goodman J., R.F. Pueschel, E.J. Jensen, S. Verma, G.V. Ferry, S.D. Howard, S.A. Kinner, and D. Baumgardner, 1998 - Shape and size of contrail ice particles - *Geophys. Res. Let*., v.25, pp.1327-1330

Han W., K. Stamnes, and D. Lubin, 1999 - Remote sensing of surface and cloud properties in the Arctic from AVHRR measurements - *J. Appl. Meteorol*., v.38, pp.989-1012

Heymsfield A.J., 1975 - Cirrus uncinus generating cells and the evolution of cirroform clouds. Part I: Aircraft observations of the growth of the ice phase - *J. Atmos. Sci.*, v.32, pp.798-808

Heymsfield A.J. and C.M.R. Platt, 1984 - A parameterisation of the particle size spectrum of ice clouds in terms of the ambient temperature and the ice water content - *J. Atmos. Sci*., v.41, pp.846-855

Houze Jr. R.A, 1981 - Structures of atmospheric precipitation systems: A global survey - *Radio Sci.*, v.16, pp.672-689

Isaacs R.G. and G. Deblonde, 1987 - Millimetre wave moisture sounding: The effect of clouds - *Radio Sci.,* v.22, pp.367-377

Klein M. and A.J. Gasiewski, 1998 - The sensitivity of millimetre and submillimeter frequencies to atmospheric temperature and water vapour variations - *IGARSS'98,* Seattle, pp.568-571

Lawson R.P., A.J. Heymsfield, S.M. Aulenbach, and T.L. Jensen, 1998 - Shapes, sizes and light scattering properties of ice crystals in cirrus and a persistent contrail during SUCCESS - *Geophys. Res. Let*., v.25, pp.1331-1334

Lee T.F., 1995 - Images of precipitation signatures from DMSP SSM/T2, SSM/I, and OLS - *J. Appl. Meteorol.,* v.34, pp.788-793

Liou K.-N., 1986 - Influence of cirrus clouds on weather and climate processes: A global perspective - *Month. Weath. Rev.,* v.114, pp.1167-1199

Liou K.-N., Y. Takano, and Ping Yang, 2000 - Light scattering and radiative transfer in ice crystal clouds: Application to climate research - *Light Scattering by Nonspherical Particles*: *Theory, Measurements, and Applications, eds. M. I. Mishchenko, J. W. Hovenier, and L. D. Travis*, Academic Press, pp.417-449

Liu G. and J.A. Curry, 1996 - large-scale cloud features during January 1993 in the North Atlantic Ocean as determined from SSM/I and SSM/T2 observations - *J. Geophys. Res.*, v.101, pp.7019-7032

Liu G. and J.A. Curry, 1998 - Remote sensing of ice water characteristics in tropical clouds using aircraft microwave measurements - *J. Appl. Meteorol.,* v.37, pp337-355

Lutz R., T.T. Wilheit, J.R. Wang, R.K. Kakar, 1991 - Retrieval of atmospheric water vapour profiles using radiometric measurements at 183 and 90 GHz - *IEEE Trans. Geosci. Remote Sensing,* v.29, pp.602-609

Matrosov S. Y., 1997 - Variability of microphysical parameters in high-altitude ice clouds: Results of the remote sensing method - *J. Appl. Meteorol*., v.36, pp.633-648

McFarquhar G.M. and A.J. Heymsfield, 1996 - Microphysical characteristics of three anvils sampled during the central equatorial pacific experiment - *J. Atmosph. Sci.,* v.53, pp.2401-2423

McFarquhar G.M. and A.J. Heymsfield, 1997 - Parameterisation of tropical cirrus ice crystal size distributions and implications for radiative transfer: Results from CEPEX - *J. Atmos. Sci.*, v.54, pp.2187-2200

McMillin L.M. and M.G. Divakarla, 1999 - Effects of possible scan geometries on the accuracy of satellite measurements of water vapour - *J. Atmos. Oceanic Technol.,* v.16, pp.1710-1721

Miao J., 1998 - Retrieval of atmospheric water vapour content in polar regions using spaceborne microwave radiometry - *Reports on Polar Research, No. 289/98,* Alfred Wegener Institute for Polar and Marine Research, Bremerhaven, Germany

Noone K.B., K.J. Noone, J. Heintzenberg, J. Stroem, and J.A. Ogren, 1993 - In situ observations of cirrus cloud microphysical properties using the counterflow virtual impactor - *J. Atmos. Oceanic Technol.,* v.10, pp.294-303

Ou S.C., K.-N. Liou, W.M. Gooch, and Y. Takano, 1993 - Remote sensing of cirrus cloud parameters using advanced very-high-resolution radiometer 3.7 and 10.9 µm channels - *Appl. Opt.,* v.32, pp.2127-2180

Ou S.C., K.-N. Liou, and T.R. Caudill, 1998 - Remote sensing of multilayer cirrus cloud systems using AVHRR data collected during FIRE-II-IFO - *J. Appl. Meteorol.,* v.37, pp.241-254

Racette P., R.F. Adler, J.R. Wang, A.J. Gasiewski, D.M. Jackson, and D.S. Zacharias, 1996 - An airborne millimeter-wave imaging radiometer for cloud, precipitation, and atmospheric water vapour studies - *J. Atmos. Oceanic Technol.,* v.13, 610-619

Rothman L.S. et al., 1998 - The HITRAN molecular spectroscopic database and HAWKS (HITRAN Atmospheric Workstation): 1996 Edition - *J. Quant. Spectrosc. Radiat. Transfer,* v.60, pp.665-710

Sassen K., 1994 - Advances in polarization diversity lidar for cloud remote sensing - *Proceed. IEEE*, v.82, pp.1907-1914

Simmer C., 1994 - Satellitenfernerkundung hydrologischer Parameter der Atmosphäre mit Mikrowellen. - Verlag Dr. Kovãc.

Wang J., W.C. Boncyk and A.K. Sharma, 1993 - Water vapour profiling over ocean surface from airborne 90 and 183 GHz radiometric measurements under clear and cloudy conditions - *IEEE Trans. Geosci. Remote Sensing,* v.31, pp.853-858

Wang J., S.H. Melfi, P. Racette, D.N. Whiteman, L.A. Chang, R.A. Ferrare, K.D. Evans, and F.J. Schmidlin, 1995 - Simultaneous measurements of atmospheric water vapour with MIR, Raman lidar and rawinsondes - *J. Appl. Meteorol.,* v.34, pp.1595-1607

Wang J., J. Zhan, P. Racette, 1997a - Storm-associated microwave radiometric signatures in the frequency range of 90-200 GHz – *J. Atmosph. Ocean. Technol*., v.14, pp.13-31

Wang J., J.D. Spinhirne, P. Racette, L.A. Chang and W.D. Hart, 1997b - The Effect of clouds on water vapour profiling from the millimeter-wave radiometric measurements - *J. Appl. Meteorol*., v.36, pp.1232-1244

Wang J. and L.A. Chang, 1998a - Profiling of atmospheric water vapour from the SSM/T2 radiometric measurements - *IGARSS'98*, Seattle, pp.2175-2177

Wang J., P. Racette, J.D. Spinhirne, K.F. Evans, and W.D. Hart, 1998b - Observation of cirrus clouds with airborne MIR, CLS, and MAS during SUCCESS - *Geophys. Res. Let.*, v.25, pp.1145-1148

Wang J., J. Zhan, and P. Racette, 1998c - Multiple aircraft microwave observations of storms over the western Pacific Ocean - *Radio Sci.*, v.33, pp.351-368

Wang J., G. Liu, J. D. Spinhirne, P. Racette, and W.D. Hart, 1999 - Observations and retrievals of cirrus cloud parameters using multichannel millimeter-wave radiometric measurements. *Submitted to J. Geophys. Res.*

Wang P.-H. P. Minnis, M.P. McCormick, G.S. Kent, and K.M. Skeens, 1996 - A 6-year climatology of cloud occurrence frequency from stratospheric aerosol and gas experiment II observations (1985-1990) - *J. Geophys. Res.* , v.101, pp.29,407-29,429

Wilheit T.T., A.T.C. Chang, J.L. King, E,B. Rodgers, R.A. Nieman, B.M. Krupp, A.S. Milman, J.S. Stratigos, and H. Siddalingaiah, 1982 - Microwave radiometric observations near 19.35, 92 and 183-GHz of precipitation in tropical storm Cora - *J. Appl. Meteorol*., v.21, pp.1137-1145

Wilheit T.T., 1990 - An algorithm for retrieving water vapour profiles in clear and cloudy atmospheres from 183-GHz radiometric measurements: Simulation studies - *J. Appl. Meteorol.,* v.29, pp.508-515

Wilheit T.T. and K.D. Hutchison, 1997 - Water vapour profile retrievals from SSM/T2 data constrained by infrared-based cloud parameters - *Int. J. Remote Sensing,* v.18, pp.3263-3277